Acta Astronautica 66 (2010) 391 – 400

Contents lists available at ScienceDirect

Acta Astronautica

journal homepage: www.elsevier.com/locate/actaastro

Human–robotic symbiosis to enable future planetary extravehicular activity

Shane E. Jacobs*, David L. Akin

Space Systems Laboratory, Department of Aerospace Engineering, University of Maryland, College Park, MD 20742, USA

ARTICLE INFO

Article history:
Received 31 January 2009
Received in revised form
3 June 2009
Accepted 30 June 2009
Available online 21 July 2009

Keywords:
Extravehicular activity
Space suits
Parallel manipulators
Exploration

ABSTRACT

This paper presents the concept of a morphing upper torso, a pressure suit design which incorporates robotic elements to enable a resizable, highly mobile and easy to don/doff spacesuit. The torso is modeled as a system of interconnected parallel manipulators, which allows the critical suit dimensions to be reconfigured to match the wearer. The back hatch of a rear-entry torso is interconnected with the waist ring, helmet ring and two scye bearings. Half-scale and full-scale experimental models are used along with analytical models to examine the implications of ring interconnections, the role of external forces generated by pressurized fabric, and the mobility of the system. The kinematics of the system are calculated, and the Jacobian matrix for the robotic system, which relates the total twist vector of the system to the vector of actuator velocities, is derived. This analysis enables quantification of the actuator requirements, given demanded trajectories of the rings. The analytical and experimental results demonstrate that the torso components can be accurately repositioned to different desired configurations. The results show that the torso could be expanded to facilitate donning and doffing, and then contracted to match different wearer's body dimensions. The demonstrated feasibility of the morphing upper torso concept makes it an exciting candidate for inclusion in a future planetary suit architecture.

1. Introduction

As the human race looks to return to the Moon and send humans to the surface of Mars, there is a growing need for a highly mobile planetary exploration pressure suit. New suit architectures must be developed to enable astronauts to explore these environments on long-duration extravehicular activity (EVA) sorties. The design of such a suit is a tremendous challenge, as the engineer is faced with a multivariable design space with complex tradeoffs between mobility, resizability, mass, don/doffability, manufacturability, modularity, stowage volume, and cost, among others. Historically, optimization of one of these variables results in compromising one or more of the others.

Maximizing mobility in a pressure suit is paramount to enable astronauts to perform a wide array of tasks without fatiguing. Working within the pressurized volume of the suit requires strength and endurance, as the pressurized fabric increases the required joint torques [1,2], making even simple tasks difficult and tiring. Soft goods engineers have developed methods of reducing these additional joint torques through the use of innovative joint designs such as the rolling convolute, the toroidal mobility joint and the flat-panel joint, all of which attempt to maintain the volume of the joint throughout the arc of joint rotation, thereby reducing the work done to bend the joint. A constant volume joint has also been achieved through the use of all hard suits, such as the AX-5, in which sets of cleverly angled rotary bearings provide the required joint mobility [2,3].

In all cases, the induced joint torques are minimized and the mobility of the suit maximized if the fit of the suit matches the anthropomorphic dimensions of the crew member. The dimensions of a future crew will likely be quite

* Corresponding author. Tel.: +1 301 405 4454.
E-mail addresses: shane@ssl.umd.edu (S.E. Jacobs), dakin@ssl.umd.edu (D.L. Akin).

0094-5765/$ - see front matter © 2009 Elsevier Ltd. All rights reserved.
doi:10.1016/j.actaastro.2009.06.017

Nomenclature

α	angle of rotation about the ring-centered x-axis
β	angle of rotation about the ring-centered y-axis
γ	angle of rotation about the ring-centered z-axis
η_i	angle that defines location of the i th node in the ring centered frame
$\vec{\Omega}$	angular velocity vector
$\vec{\Theta}$	Euler angles $=[\alpha,\beta,\gamma]^T$
BH	back hatch
EMU	extravehicular mobility unit
EVA	extravehicular activity
$\vec{F}_1$	vector of applied forces on the helmet ring
$\vec{G}$	location of the center of the helmet, which serves as the origin of the helmet coordinate frame
$H=(\vec{G},\hat{u},\hat{v},\hat{w})$	helmet ring-centered frame
HUT	hard upper torso
$I=(\vec{O},\hat{x},\hat{y},\hat{z})$	inertial frame
J	Jacobian matrix which multiplies the total twist vector $\dot{\vec{X}}$ of the system to yield the vector of actuator velocities $\dot{\vec{l}}$
$\vec{L}$	vector function of link length equations
$\dot{\vec{l}}$	vector of actuator velocities $=[\dot{l}_1,\dot{l}_2\ldots,\dot{l}_n]^T$
$\vec{l}_k$	vector describing the k th linkage
$\lvert\vec{l}_k\rvert$	length of the k th linkage
LS	left shoulder
$\vec{M}_1$	vector of applied moments on the helmet ring
MUT	morphing upper torso
n	total number of linkages
NASA	National Aeronautics and Space Administration
$\vec{O}$	origin of the base frame $=[0,0,0]^T$
${}^H\vec{p}_{i/G}$	location of the i th node relative to the center of the ring $\vec{G}$, written in the local ring-centered frame (H) coordinates
${}^I\vec{p}_{i/O}$	location of the i th node relative to the center of the back hatch $\vec{O}$, written in the inertial frame (I) coordinates
PLSS	portable life support system
Pose	combination of position and orientation
psi	pounds per square inch
$\vec{q}_{act}$	vector of actual link lengths
$\vec{q}_{meas}$	vector of measured node-to-node distances
$\vec{q}_{ref}$	vector of reference node-to-node distances
${}^IR_H$	rotation matrix required to rotate a vector from the ring-centered coordinate frame H to the inertial frame I
RS	right shoulder
Scye	armhole in the torso section of a garment
$\hat{s}_k$	unit vector along the k th linkage
SUT	soft upper torso
$\vec{T}$	vector of link tensions
Twist	combination of linear and angular velocity
${}^I\vec{v}_G$	linear velocity of point $\vec{G}$
$\vec{W}$	combined vector of wrenches applied to all four rings
$\vec{W}_1$	helmet ring wrench
Wrench	combination of forces and moments
$\vec{X}$	combined pose of the four rings
$\dot{\vec{X}}$	combined twist of the four rings
$\vec{X}_0$	initial guess of pose for forward kinematics
$\vec{x}_1$	pose of the helmet ring
$\dot{\vec{x}}_1$	twist of the helmet ring
$\vec{X}_{act}$	actual pose of the experimental model
$\vec{X}_{ref}$	reference pose of the experimental model

varied. NASA has laid out standards for all crewed vehicles and interfaces [4,5] that require accommodation from the 5th percentile American female to the 95th percentile American male. In some cases, systems can be designed to accommodate the extreme case (a bed that accommodates the 95th percentile male, for example, will work for everyone), while other systems must incorporate adjustability and resizability, or have several sizes of each component.

The wide range of crew member size especially affects suit design, as each crew member needs a suit that fits precisely. Unfortunately, the closer the fit, the more unique each suit becomes, complicating issues of fabrication and support logistics, and increasing costs. During the Apollo program, each astronaut had custom-made suits. This eliminated all possibilities of flexibility in fitting old suits to new astronauts, and clearly increased manufacturing, maintenance and repair costs. This architecture aimed to maximize mobility through a close fit, but even this approach was imperfect, as it became apparent that it was difficult to compensate for body shape changes in varying gravity levels. The modular system employed in the EMU uses various sizes of each component, which can be assembled into many different combinations, guaranteeing a fairly close match to each astronaut [6]. This reduces production costs and increases flexibility and interchangeability, but at the cost of reduced mobility due to inexact fit.

Another challenge of pressure garment design is that this critical feature that makes the suit highly usable (a close fit to body dimensions) makes it difficult to ingress and egress. An examination of various suit-entry types for hard upper torso (HUT) architectures (such as that used in the extravehicular mobility unit, EMU) has shown that each presents its own compromises between suit fit and don/doffability [7]. An illustration of this compromise is the inter-scye dimension in waist-entry suits (scye is the term used by garment designers to refer to the armhole in the torso section), which must be large enough to allow ingress, causing

misalignment of the scye bearing and the shoulder, and therefore reducing shoulder mobility. This is a current issue with the EMU.

Pressure suit design specifically for planetary exploration is further complicated by the fact that the suits must be light enough for an astronaut to traverse the surface for many hours while bearing the weight of the suit and portable life support system (PLSS). The feasibility of all-hard suits for planetary exploration is clearly limited by this lightweight requirement. Completely soft suits which utilize soft upper torsos (SUT), such as the A7L and A7LB used to explore the Moon during the Apollo missions, are much lighter, can be stowed in a smaller volume, and could provide the baseline for the next generation planetary suit. However, the limited mobility of these suits severely restricted the Apollo astronauts, and must be improved upon for the next planetary exploration missions.

Several designs have been proposed, tested, and utilized in field trials to isolate these difficult problems and examine possible solutions. Each year NASA performs a series of experiments [8–10] using two such concepts, the Mark III and the I-Suit [11]. Each of these suits has been shown to be extremely valuable and provides the wearer with a great deal of mobility and exploration capability. However, it is clear from these field trials that there remains the need for advanced space suit architectures to enable the type of exploration envisioned for the coming decades.

To date there is no solution to the challenge of making a suit resizable, highly mobile, lightweight, minimal stowage volume, and easy to ingress/egress. In light of these challenges, new and different suit architectures must be developed to enable astronauts to explore the Moon and Mars. The concept proposed here is the morphing upper torso (MUT); a soft pressure garment that does not compromise mobility nor don/doffability. It has the potential to be lightweight, resizable, easy to ingress/egress, and fit precisely a wide range of astronauts.

2. MUT concept

The proposed MUT architecture is a soft upper torso pressure garment with dimensions that can be dynamically reconfigured to match the wearer's body shape and motions. This requires manipulating the position and orientation (hereafter referred to as the "pose") of the waist ring, helmet, and scye bearings. The scye bearings are the bearings that provide shoulder rotation, and their pose is especially critical, as if their center of rotation is not exactly collocated with the center of rotation of the shoulder, the astronaut's upper arm mobility will be severely limited. The helmet–waist distance is another critical sizing parameter; too short and it is extremely uncomfortable, too long and the subject loses waist mobility and/or field of view. The capability to dynamically finely tune the pose of these four rings enables a closely fitting suit without customizing each suit and without sacrificing don/doffability.

The concept of highly adjustable scye bearings was developed by Graziosi et al. [12]. High strength linear actuators were attached across the front and back of a waist entry SUT, demonstrating that the bearings could be widely

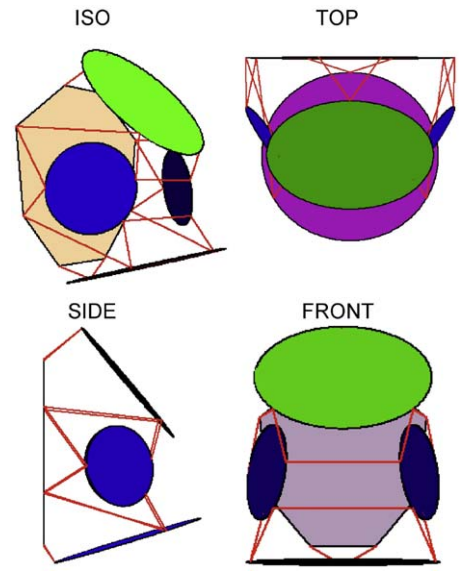

Fig. 1. Four views of the interconnected morphing upper torso design. The straight lines represent actuated tensile linkages, which can reposition the helmet, waist, and scye bearings.

spaced during donning and doffing, and then repositioned to a much narrower configuration during wear. This would allow the bearing to be accurately collocated with the center of rotation of the wearer's shoulder, maximizing shoulder mobility, without hindering donning and doffing.

This unique concept is furthered in this work by extending the manipulability of the scye bearings to the entire torso assembly. The helmet, two scye bearings, and waist bearing are connected with adjustable linkages to form a system of interconnected parallel manipulators. Parallel manipulators are used in situations which require fine positioning, high stiffness and operation under high load, but are confined to small workspaces [13–16]. Incorporating parallel robotics into suit design seems to be a logical design choice, as the strengths and capabilities of parallel manipulators map well to the requirements of a reconfigurable torso. The high pressure forces on the helmet, waist and scye rings create high loads. Additionally, while the physical dimensions of humans vary greatly, they all lie within a workspace that is compatible with a parallel manipulator. Finally, high accuracy and stiffness are clearly demanded, as the rings must exactly match the astronaut's dimensions to make for a highly mobile suit.

By connecting each ring of the suit as a parallel manipulator with a set of adjustable linkages, as shown in Fig. 1, the pose of each ring can be manipulated to match the wearer's dimensions and movements. The rings are both connected to the back hatch, which serves as an inertial ground, and interconnected to each other. Thus some linkages interconnect two moving rings. This human–robotic symbiosis—the confluence of robotics and pressure suit design—enables a resizable and highly mobile spacesuit.

The MUT concept can be integrated in five progressive implementations, as outlined below. Each represents an

incremental step in the morphing technology, providing enhanced capabilities over the previous system.

1. *Manual static*: Links are lengthened during donning and doffing, then manually reset to desired individual dimensions prior to pressurization. This enables one suit to precisely fit multiple users. High strength actuators are not required; instead, a simple, low-mass, hand-adjustable mechanism can be used to change the link lengths. While the next four implementations require some incremental advances in actuator technology, this passive static implementation is simple and feasible in the near term. It is a low-mass, low-complexity solution to many of the aforementioned problems facing suit designers. In fact, this system could actually fit each wearer better than custom-made suits, as suit dimensions could be fine-tuned to accommodate body shape changes (due to different g-levels) that occur between the time the subject is fitted and the time of the EVA. Given a long-duration trip to Mars, each crew member's body shape will almost certainly change with time. Elongation of the spine can be expected during exposure to microgravity en route, amongst other possible changes. This passive static system would ensure that the dimensions critical to suit mobility could adapt to match these changes.
2. *Active static*: Links can be adjusted after pressurization, providing quick modifications for comfort, and enabling fine control of suit dimensions at any time, while the suit is pressurized. This does not impose any additional complexity onto the life support system (nor do any of the implementations), as a back pressure regulator, similar to those used in the EMU and other EVA suits, would be sufficient to maintain the correct pressure in the suit. The primary challenge of the active pressurized system though is that it requires small, low-mass, high force, large stroke, in-line actuators. These add mass and complexity, and require power, so the benefits of the MUT must outweigh these costs.
3. *Active reconfigurable*: The suit can be set to specific configurations for each task. For example, the suit could be dynamically adjusted to dimensions optimal for walking, kneeling, or sitting. This implementation is easy to envision if the active pressurized system has been achieved, as the actuators can adjust the suit dimensions while the suit is pressurized.
4. *Active adaptive*: The suit continually adjusts to the wearer's body kinematics in real time. For example, as the subject brings their arms together, the scye bearings move inwards to compensate. As the subject bends over, the angle of the waist adjusts to aid the motion. This would provide maximum mobility and flexibility, as the suit would move with the subject, essentially staying out of the way of the subject as they move. This active adaptive system would eliminate work done "against" the suit, allowing the crew member to explore as if they were in a shirt sleeve environment. This requires not only the actuators described in the active pressurized system, but real-time control algorithms, using information about the astronaut's actual positions and velocities, to continuously adjust the suit's dimensions.
5. *Active enhanced*: This system represents atruly robotically augmented suit, which would not only reduce the induced joint torques and workspace restrictions as in the active adaptive system, but could in fact give the astronaut enhanced strength, with the suit acting as an exoskeleton. While wearing this suit the subject would, for example, be able to carry larger loads than they could while not wearing the suit. The robotic system would not only offset the weight of itself, but go one step further by providing the crew member enhanced abilities. This system also requires real-time control algorithms as well as actuators with even greater force capability than required in the active adaptive system.

3. Analytical models

Kinematic and dynamic models were made of the robotic system to analyze and evaluate the MUT concept. The derivations are presented below, and then the mathematical simulations are used in conjunction with the experimental models to demonstrate the feasibility of the concept.

3.1. Kinematics

The inverse kinematics transformation is the calculation of the link lengths given a desired pose of the four rings. The forward kinematics is the opposite transformation, calculating the pose of the rings from a set of link lengths. Derivation of the kinematics model for a generic MUT was performed as follows: vectors are represented with an arrow $\vec{}$, and unit vectors are represented with a hat $\hat{}$.

An inertial frame $I = (\vec{O}, \hat{x}, \hat{y}, \hat{z})$ is attached to the center of the back hatch, with origin $\vec{O} = [0,0,0]^T$, and moving coordinate frames are attached to the center of each of the four rings. For example, the helmet ring coordinate system is defined as $H = (\vec{G}, \hat{u}, \hat{v}, \hat{w})$, where $\vec{G}$ is the location of the center of the helmet ring. The helmet will be used as an example throughout this derivation, but it is understood that there are also right shoulder, left shoulder, and waist coordinate frames. The location of the origins of these frames at the center of each ring makes for simple determination (and input) of commonly used dimensions such as inter-scye distance.

The attachment points for each linkage are defined as nodes. There are three nodes on each of the four rings; nodes 1–3 are located around the perimeter of the helmet ring, 4–6 on the right shoulder ring (RS), 7–9 on the left shoulder ring (LS), 10–12 on the waist ring, and nodes 13–20 are attached to the perimeter of the back hatch (BH). The nominal set of linkages and their numerical assignments, along with the nodes which each link interconnects are listed in Table 1. This set of linkages, which corresponds to Fig. 1, is just one example of the many configurations under examination. Ultimately the system will be optimized to minimize the number of linkages while maintaining controllability of the required degrees of freedom. The analytical models are derived for an arbitrary set of linkages such that they can be used in all cases.

The position vector ${}^I\vec{p}_{i/O}$ defines the location of the i th node relative to the center of the back hatch $\vec{O}$, written in the

Table 1
Node and linkage assignments.

Link	Node 1	Node 2	Physical location
1	1	13	Helmet-BH
2	1	20	Helmet-BH
3	2	9	Helmet-LS
4	2	14	Helmet-BH
5	3	4	Helmet-RS
6	3	19	Helmet-BH
7	4	9	RS-LS
8	5	8	RS-LS
9	5	12	RS-Waist
10	6	18	RS-BH
11	6	19	RS-BH
12	7	14	LS-BH
13	7	15	LS-BH
14	8	10	LS-Waist
15	10	15	Waist-BH
16	11	16	Waist-BH
17	11	17	Waist-BH
18	12	18	Waist-BH

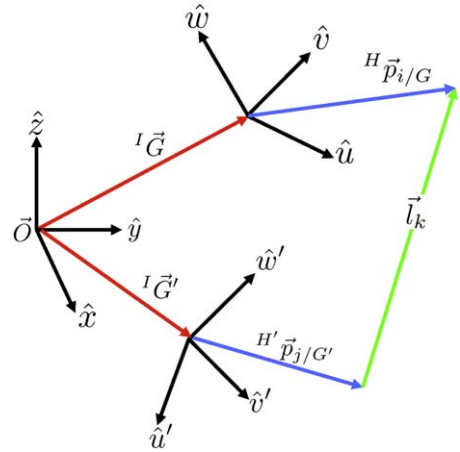

Fig. 2. Visual representation of Eq. (4).

inertial frame (I) coordinates. The nodes physically attached to the back hatch are already in the base frame. The position vector $^H\vec{p}_{i/G}$ defines the i th node relative to the center of the ring $\vec{G}$, written in the local ring-centered frame (H) coordinates. As each ring is modeled as a circle in the x–z plane of the ring, these nodes are actually defined by one angle each, η_i, where $^H\vec{p}_{i/G} = [\cos\eta_i, 0, \sin\eta_i]^T$. Defining the nodes in this way allows easy manipulation of the location of the node on the ring by simply adjusting η_i.

The position of each ring is defined by the vector from the origin of the inertial frame to the origin of the ring-centered frame, i.e. simply $^I\vec{G}$. The orientation of each ring is defined by three Euler angles, $\vec{\Theta} = [\alpha, \beta, \gamma]^T$, i.e. rotation of γ about the z-axis, rotation of β about the ring centered y-axis, and rotation of α about the ring-centered x-axis. The pose of the helmet ring is given by

$$\vec{x}_1 = \begin{bmatrix} ^I\vec{G} \\ \vec{\Theta} \end{bmatrix} = \begin{bmatrix} G_x \\ G_y \\ G_z \\ \alpha \\ \beta \\ \gamma \end{bmatrix} \tag{1}$$

A rotation matrix from the ring frame H to the inertial frame I, ^IR_H is constructed from the three Euler angles, as shown below:

$$^IR_H = \begin{bmatrix} c\beta c\gamma & s\alpha s\beta c\gamma - c\alpha s\gamma & c\alpha s\beta c\gamma + s\alpha s\gamma \\ c\beta s\gamma & s\alpha s\beta s\gamma + c\alpha c\gamma & c\alpha s\beta s\gamma - s\alpha c\gamma \\ -s\beta & c\beta s\alpha & c\beta c\alpha \end{bmatrix} \tag{2}$$

where c is the shorthand for cos and s is the shorthand for sin. Thus the position vector of the i th node, relative to the ring center $\vec{G}$, written in the inertial frame coordinates is given by

$$^I\vec{p}_{i/G} = {}^IR_H\,{}^H\vec{p}_{i/G} \tag{3}$$

Once all nodes have been written in the inertial frame using Eq. (3), the loop vector equations can be written for each of the linkages:

$$(^I\vec{G} + {}^I\vec{p}_{i/G}) - (^I\vec{G}' + {}^I\vec{p}_{j/G'}) = \vec{l}_k \tag{4}$$

where $\vec{l}_k$ is the vector from node j to node i, $k = 1, 2, \ldots, n$ and n is the number of linkages. Note that for nodes on the back hatch, $\vec{G}' = \vec{O} = \vec{0}^T$, while for linkages that interconnect two moving rings, $\vec{G}'$ represents the origin of the ring on which the j th node lies. This is one of the key differences between this derivation and the standard derivation for a typical parallel manipulator, and is the primary complicating factor in these equations. Fig. 2 shows a visual representation of the loop vector equations.

The inverse kinematics can be directly calculated by solving Eq. (4) for the magnitudes of $\vec{l}_k$. These equations are determinate and uncoupled, thus each linkage length can be solved independently.

The forward kinematics are not as straightforward because they require solving a large system of coupled, nonlinear equations with transcendental terms. This complex system of equations can be solved using numerical methods such as the Newton–Raphson method. This numerical technique will yield a solution for the pose of the four rings given an initial guess for the overall pose. As the approximate pose of the entire system is known *a priori*, this initial guess is a good starting point for the system to converge to the actual pose. This technique makes no attempt to solve for all the possible poses given the set of link lengths, but rather converges to one solution for the actual pose.

Let $\vec{X}$ be the vector of 24 unknowns (three position coordinates and three orientation coordinates for each of the four rings), i.e. the combined pose of the four rings. Let $\vec{L}$ be the vector function of the link length equations and $|\vec{l}_k|$ is the known length of link k. A vector function $\vec{f}(\vec{X})$ is defined as

$$f_k(\vec{X}) = L_k^T L_k - |\vec{l}_k|^2 \tag{5}$$

for each k from 1 to n. This is equivalent to

$$f_k(\vec{X}) = ((^I\vec{G} + {}^I\vec{p}_{i/G}) - (^I\vec{G}' + {}^I\vec{p}_{j/G'}))^T \bullet ((^I\vec{G} + {}^I\vec{p}_{i/G}) - (^I\vec{G}' + {}^I\vec{p}_{j/G'})) - |\vec{l}_k|^2 \tag{6}$$

The solution is the set of positional and orientation coordinates of the rings such that

$$f_k(\vec{X}) = 0, \quad \forall k \tag{7}$$

Setting the initial guess for the pose as $\vec{X}_0$, and at each subsequent iteration setting $\vec{X}_0 = \vec{X}$, Eq. (8) can be iterated to solve the system of equations for $\vec{X}$ such that Eq. (7) is satisfied within a numerical tolerance:

$$\vec{X} = \vec{X}_0 - [F'(\vec{X}_0)]^{-1}\vec{f}(\vec{X}_0) \tag{8}$$

where F' is the matrix of partial derivatives of each function f_k with respect to each variable in $\vec{X}$. This method is only valid when F' is square and invertible.

3.2. Jacobian derivation

The Jacobian matrix relates the velocities of the actuators to the velocities of the rings, which is critical for the dynamic model. To derive the Jacobian, the vector of actuator velocities is defined as $\dot{\vec{l}} = [\dot{l}_1, \dot{l}_2, \ldots, \dot{l}_n]^T$ and the vector $\dot{\vec{x}}_1$ is defined as the "twist" of the helmet ring, which is the combination of the linear velocity ${}^I\vec{v}_G$ of a point on the platform, (this point is known as the operating point, in this analysis it is taken as the center of the ring which also coincides with the origin of the ring frame, $\vec{G}$) and the angular velocity vector ${}^I\vec{\Omega}$. Eq. (9) shows the definition of the twist vector for the helmet ring, $\dot{\vec{x}}_1$, which is a 6×1 vector:

$$\dot{\vec{x}}_1 = \begin{bmatrix} {}^I\vec{v}_G \\ {}^I\vec{\Omega} \end{bmatrix} \tag{9}$$

Similar vectors are made for the two shoulder rings and the waist ring, and the total twist vector $\dot{\vec{X}}$ of the system is the 24×1 concatenation of these four twist vectors, $\dot{\vec{X}} = [\dot{\vec{x}}_1, \dot{\vec{x}}_2, \dot{\vec{x}}_3, \dot{\vec{x}}_4]^T$.

The next step requires the transport equation:

$${}^I\dot{\vec{p}}_{i/G} = {}^IR_H\,{}^H\dot{\vec{p}}_{i/G} + {}^I\vec{\Omega} \times {}^I\vec{p}_{i/G} \tag{10}$$

where ${}^H\dot{\vec{p}}_{i/G}$ is clearly equal to 0 as the nodes are fixed to the ring.

All variables are now in the inertial frame, so the prefix ^{I} will hereafter be omitted. Differentiating Eq. (4) with respect to time and using Eq. (10), yields

$$\hat{s}_k \bullet (\vec{v}_G - \vec{v}_{G'}) + (\vec{p}_{i/G} \times \hat{s}_k) \bullet \vec{\Omega} - (\vec{p}_{j/G'} \times \hat{s}_k) \bullet \vec{\Omega}' = \dot{l}_k \tag{11}$$

The notations $\vec{v}_{G'}$ and $\vec{\Omega}'$ refer to the cases when the jth node is on another moving ring and each ring has a twist. As in Eq. (4), the equations become much simpler for linkages that connect a ring to the back hatch, as $\vec{v}_{G'} = \vec{0}^T$ and $\vec{\Omega}' = \vec{0}^T$.

Writing Eq. (11) for each $k = 1, 2, \ldots, n$ and combining and arranging in matrix form yields

$$J\dot{\vec{X}} = \dot{\vec{l}} \tag{12}$$

Therefore, J is an $n \times 24$ matrix, which multiplies the total twist vector $\dot{\vec{X}}$ of the system to yield the vector of actuator velocities $\dot{\vec{l}}$. It should be noted that this Jacobian matrix J corresponds to the inverse Jacobian for a serial manipulator, and in some notations is written as J^{-1} [15].

3.3. Static analysis

The Jacobian derived above can also be used to relate the tensile forces in the linkages to the forces and moments applied to the rings. The vector $\vec{W}_1$ is referred to as the "wrench", which is defined as

$$\vec{W}_1 = \begin{bmatrix} \vec{F}_1 \\ \vec{M}_1 \end{bmatrix} \tag{13}$$

where $\vec{F}_1$ is the vector of applied forces and $\vec{M}_1$ is the vector of applied moments. Again concatenating the four 6×1 wrench vectors into the 24×1 wrench vector of the total system yields $\vec{W} = [\vec{W}_1, \vec{W}_2, \vec{W}_3, \vec{W}_4]^T$. Let $\vec{T}$ be the $n \times 1$ vector of link tensions, and the two are related by

$$\vec{W} = J^T\vec{T} \tag{14}$$

4. Experimental models

Several experimental models were designed and manufactured to investigate the accuracy of the analytical model and feasibility of the MUT concept. First a small-scale MUT was created for initial experiments. The MUT was designed with five test plugs (back hatch, helmet, waist, and two scye rings) integrated into a urethane-coated nylon pressure bladder and nylon restraint layer.

While traditional SUTs are shaped and sized by their fabric pattern, the MUT soft goods were designed with additional material to ensure that the linkages were fully responsible for positioning the MUT plates. Therefore, in the unwired configuration of the MUT, the waist, helmet, and scye rings are not at specific angles or locations, rather there is enough space to allow the MUT to be manipulated into various configurations.

For initial static and kinematic analysis, a system of manually adjustable links was created and integrated into the small scale MUT. Fig. 3 shows the configuration of the links on the model.

Fig. 3. Side view of the small scale experimental MUT lying on its back.

Fig. 4. Experimental model for the isolation of pressurized fabric effects.

Fig. 5. Full scale MUT model in expanded state (left) and reconfigured to nominal configuration (right).

A second experimental model was created to examine the role of the pressurized fabric on the MUT system, as shown in Fig. 4. The soft goods were removed from the MUT, and a test stand was developed to support hanging weights attached to each plate. The weights are attached such that the force pulls normal to each plate, along the same vector as the force due to internal pressure in the pressurized model. This model is identical to the small scale MUT in every way, other than the removed soft goods, successfully isolating the influence of the pressurized fabric on the system.

The third experimental model is a full scale MUT, which is a modification of an I-Suit SUT which has been expanded. The I-Suit is an experimental all-soft multi-bearing space suit developed by ILC Dover LP [11]. The helmet, waist, back hatch, and scye rings implemented in the MUT are identical to those of the I-Suit. The difference lies in the soft goods, which were expanded from the baseline I-Suit dimensions. Each of the four actuated rings was displaced outwards along the normal vector, and the scye rings were canted outwards from the body centerline. This provides excess soft goods and therefore the ability to reposition and reorient the rings with the use of adjustable linkages.

The corresponding pressure bladder and restraint layer were designed, and subsequently fabricated of the same materials used in the I-Suit. The complete expanded SUT, shown on the left in Fig. 5, was then modified to produce an experimental MUT, using similar methods to those used for the construction of the small scale MUT. The fully constrained model is shown on the right of Fig. 5.

Measurements of all three experimental models were taken using a FaroArm^{TM} coordinate measuring machine capable of very high precision (± 0.1 mm) three-dimensional measurement. This enabled measurement of the exact angles and locations of the plates as well as the exact locations of the attachment points. The measurements provided an excellent means of quantitatively comparing the experimental models, and correlating the data with the analytical models. Link tensions were also experimentally measured using an in-line force transducer.

5. Results and discussion

The expanded SUT is larger than the largest sized HUT currently employed in the EMU, and as such would be easy to ingress and egress for most of the population. The initial lengths of the linkages need to be at least as long as the material dictates, to ensure this relative ease is maintained. These initial lengths were measured by pressurizing the expanded SUT and attaching linkages such that they were just taut. The link lengths were also calculated for a MUT configuration that matches that of the I-Suit SUT. This nominal I-Suit configuration represents a torso that is a relatively close fit to an average male. To truly take advantage of MUT technology, dimensions specific to each subject would be input into the model. For the purposes of demonstrating the feasibility of the MUT, however, the ability to reconfigure to the I-Suit dimensions was chosen as the nominal reconfiguration.

The inverse kinematics model is used to calculate the node-to-node distances for various torso configurations. These calculated link lengths, though, have some inherent error, as they are linear distances and do not compensate for the added lengths required to bend around the pressurized torso. This difference between the vector of node-to-node distances $\vec{q}_{meas}$, and the vector of actual link lengths $\vec{q}_{act}$, implies that setting them equal will not reconfigure the MUT to the desired pose $\vec{X}_{ref}$. To solve this problem, an iterative method was developed, which uses both the experimental model and the inverse kinematics model, to obtain a set of actual link lengths required to reconfigure the MUT to the desired pose. Fig. 6 shows visually this iterative method.

The pose of the four rings in the I-Suit configuration is represented by $\vec{X}_{ref}$, this is the desired or reference pose. This vector is input into the inverse kinematics model to obtain the vector of desired distances between nodes, denoted by $\vec{q}_{ref}$. The vector of desired distances is compared to the vector of measured distances $\vec{q}_{meas}$, and the difference is denoted by the vector of link length changes $\vec{e}$. The link lengths are changed by the requisite amount by the link space controllers, (in this case the links are adjusted by hand while the suit is unpressurized), which yields the vector of the actual link lengths $\vec{q}_{act}$. The MUT experimental model is then pressurized, and the actual pose of the rings $\vec{X}_{act}$ is obtained using the FaroArm^{TM}. The inverse kinematics model is used once again to calculate the actual node-to-node distances in the experimental model, $\vec{q}_{meas}$, and the loop is repeated until $\vec{q}_{meas} = \vec{q}_{ref}$ and $\vec{X}_{act} = \vec{X}_{ref}$. At this point, the vector of actual

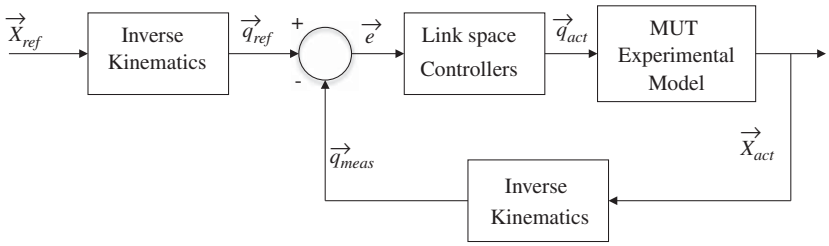

Fig. 6. Iterative method used to reconfigure the experimental MUT using the inverse kinematics model.

Table 2
Link length changes from expanded to nominal configurations.

Link	Length expanded SUT	Length nominal SUT	Change
1	13.82	9.17	−4.65
2	13.82	9.17	−4.65
3	17.17	10.59	−6.58
4	36.37	31.34	−5.03
5	17.17	10.59	−6.58
6	36.37	31.34	−5.03
7	37.24	24.82	−12.42
8	42.65	29.95	−12.70
9	19.30	14.07	−5.23
10	23.67	19.35	−4.32
11	22.20	19.84	−2.36
12	22.20	19.84	−2.36
13	23.67	19.35	−4.32
14	19.30	14.07	−5.23
15	41.43	39.01	−2.42
16	14.40	10.67	−3.73
17	14.40	10.67	−3.73
18	41.43	39.01	−2.42

All lengths in cm.

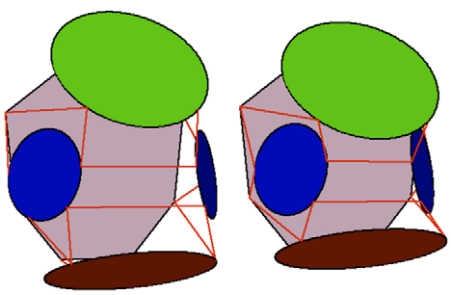

Fig. 7. Analytical model showing reconfiguration from expanded (left) to nominal (right) dimensions.

link lengths $\vec{q}_{act}$ is noted as the set of link lengths required to reconfigure the MUT to the desired pose.

Table 2 shows the changes in link lengths necessary to contract the expanded SUT to a nominal I-Suit SUT (all lengths in cm), obtained using the iterative method. Note that this configuration of links is symmetric about the *y*–*z* plane, and thus all of the links come in pairs, except for links 7 and 8 which cross the plane of symmetry, attaching the two scye bearings. Fig. 7 shows graphically the two different configurations in the analytical model.

The result is that when the length changes shown in Table 2 are applied to the full-scale MUT model, the resulting configuration of the experimental model is almost identical to that of the analytical model. The relative location of the nodes and the rings correlate very well: the inter-scye distance has been shrunk to that of the I-Suit, the waist ring has been lifted and tilted upwards, and the helmet ring brought downwards and towards the back hatch. Similar results were obtained with the inverse kinematics model and the small scale MUT, as it was successfully reconfigured into several arbitrary configurations. Thus far, measurements have shown that the configuration changes predicted by the inverse kinematics model produce similar outcomes when applied to the experimental models. This implies that a vector of actual link lengths, $\vec{q}_{act}$, could be determined *a priori* for any given suit configuration, thus enabling the suit to be resized to fit precisely any sized crew member.

Table 3
Example of measured link tensions, with MUT pressurized at 20 kPa.

Links	Tension (N)
4 and 6	520
7	596
8	476
11 and 12	556
15 and 18	654

In addition, the link length changes shown in Table 2 provide information critical to the design of the actuators, yielding a baseline for the amount of stroke necessary for each link. Clearly the actuator range requirements vary greatly, as some of the links require up to 12 cm of travel, while others require as little as 2 or 3 cm.

A force transducer was installed in-line with the linkages to record the link tensions in the full size MUT. Tensile forces in the links are a function of suit pressure, but since the operating pressure of a future planetary suit is unknown, the results presented here are for a suit pressure of 20 kPa (3 psi). Table 3 shows the measured forces in the links, which are all in the range of 440–670 N (100–150 lbs). Due to the symmetry of the nominal configuration about the *y*–*z* plane, corresponding links on either side of the suit (4 and 6, 11 and 12, 15 and 18) have the same tension. Several of the links are too short to accommodate the force transducer, so their tensions have not been experimentally measured. However, based on information from the analytical static model, and the relative correlation between the model and the linkages that were measured, it is estimated that the unmeasured link tensions are also on the order of 500 N.

The experimental models were also used to investigate the role of the pressurized fabric in the MUT system. The link lengths were maintained constant for both the pressurized and the hanging weight model, and the pose of the plates were measured and compared. Differences along the x and y axes were negligible; however, a significant difference between the two models was evident along the z-axis (pointing straight up the spine of the torso). Clearly the fabric interacts with the linkages and the plates, and this effect must be modeled analytically.

The additional fabric in the MUT, which allows the critical sizing dimensions of the torso to be adjusted, tends to bulge out when the suit is reconfigured. These bulges do not occur near the critical joint areas, and as such should not hinder suit mobility. It is critical for mobility, for example, that the scye bearings be exactly collocated with the center of rotation of the subject's shoulder, and the waist ring must be in the correct pose to provide waist mobility, but it is not critical that the fabric of the suit lie flat against the subject's midsection. The role of the pressurized fabric must be analyzed in greater detail if the MUT is to be implemented in a wearable suit, but the bulging of the excess fabric, while it may appear unsightly, should not pose a mobility problem.

6. Conclusions

The analytical and experimental investigations described herein have demonstrated the feasibility of the morphing upper torso concept. The kinematic and dynamic equations have been developed and solved, and models have been developed that predict the link tensions for any given configuration. Experimentally it has been shown that given a desired suit configuration, a calibrated inverse kinematics model can provide adequate information on link lengths to accurately control the MUT reconfiguration.

Results obtained from both experimental and mathematical models have produced preliminary actuator requirements for a powered MUT. Actuators must be low profile, yet in some cases able to change the link length by up to 12 cm. Ideally actuators will be placed in-line with the linkage; however, mounting the actuators on the backpack and utilizing a cable driven system to adjust the links is also a possibility. Potential actuation methods include electromechanical actuators, air muscles, hydraulics, and other low profile devices. These actuators must be integrated into the system in such a way that they do not encroach on the subject or hinder suit performance.

Additionally, results from the experimental models have shown that fabric tension at the SUT-plate interface plays a significant role in MUT configuration. Forces due to pressurized fabric, acting both on the SUT plates and on the linkages themselves, need to be incorporated into the analytical models.

The vision of a fully robotically augmented suit will take time to fulfill. Presently the main focus is to create a passive static system, which can both be achieved in the near-term and provide significant advances over traditional suit architectures. The final goal of this research is to develop the concept such that morphing upper torso technology can be incorporated into a planetary exploration suit. The analytical and experimental models developed in this work are a major step in that direction.

7. Future work

Future work will focus on the synthesis of the robotic design, especially optimizing the placement, number and power requirements of the linkages. Optimization techniques will be employed to minimize the additional mass and power that the actuators add to the suit. The advantages gained in mobility and resizability clearly must outweigh these costs. The challenge of controlling the system is under investigation, and several controllers are being modeled. Additionally, the interaction of the pressurized fabric with the rings and the linkages must be modeled.

It is also believed that this work can be incorporated into other components of the pressure suit assembly. The capabilities of parallel manipulators map so well to pressure suit design requirements that it is a logical progression to incorporate parallel manipulators in the arm and lower torso assemblies as well. Continued work in this area could lead to highly mobile lower torso assemblies which will be needed for long term exploration of the Moon and Mars.

Acknowledgments

This work received initial funding from ILC Dover LP and further funding from the NASA Institute for Dexterous Space Robotics. Thanks to our colleagues at the Space Systems Laboratory for their help and dedication. Thanks to Dave Graziosi and his team at ILC Dover for providing continued help and guidance. This paper was originally presented at the 59th International Astronautical Congress in Glasgow, Scotland. Sincere thanks to the Canadian Space Agency for providing the funding to attend. Finally, thanks to the anonymous reviewers for their helpful comments.

References

[1] A. Frazer, B. Pitts, P.B. Schmidt, J.A. Hoffman, D.J. Newman, Astronaut performance: implications for future spacesuit design, in: International Astronautical Congress (IAC-02-G.5.03), 2002.
[2] G.L. Harris, The Origins and Technology of the Advanced Extravehicular Space Suit, AAS History Series, vol. 24, 2001.
[3] K. Thomas, H.J. McMann, US Spacesuits, Springer, Berlin, 2006.
[4] Man–systems integration standards NASA-STD-3000, Technical Report Review B, NASA, July 1995.
[5] Constellation program human–systems integration requirements, Technical Report CxP 70024, NASA, 2006.
[6] N.C. Jordan, J.H. Saleh, D.J. Newman, The extravehicular mobility unit: a review of environment, requirements, and design changes in the US spacesuit, Acta Astronautica 59 (2006) 1135–1145.
[7] D. Graziosi, J. Ferl, K. Splawn, An examination of spacesuit entry types and the effect on suit architecture, in: Space 2004 (2004-5969), 2004.
[8] A.J. Ross, Desert research and technology studies 2005 report, in: 36th International Conference on Environmental Systems (2006-01-2138), 2006.
[9] B. Romig, J. Kosmo, A.J. Ross, C. Bernard, L. Aitchison, D.B. Eppler, K. Splawn, Desert research and technology studies 2006 report, in: 37th International Conference on Environmental Systems (2007-01-3131), 2007.
[10] B. Romig, J. Kosmo, Desert research and technology studies 2007 report, in: 38th International Conference on Environmental Systems (2008-01-2062), 2008.
[11] D. Graziosi, K. Splawn, J. Ferl, Evaluation of the rear entry i-suit during desert rats testing, in: 36th International Conference on Environmental Systems (2006-01-2143), 2006.

[12] D. Graziosi, J. Ferl, K. Splawn, Development of a space suit soft upper torso mobility/sizing actuation system, in: 34th International Conference on Environmental Systems (2004-01-2342), 2004.
[13] D. Stewart, A platform with six degrees of freedom, Proceedings of the Institution of Mechanical Engineers 180 (15) (1965) 371–378.
[14] L.-W. Tsai, Robot Analysis: The Mechanics of Serial and Parallel Manipulators, Wiley, New York, 1999.
[15] J.-P. Merlet, Parallel Robots, Solid Mechanics and its Applications, second ed., vol. 128, Springer, Berlin, 2006.
[16] B. Dasgupta, T. Mruthyunjaya, The stewart platform manipulator: a review, Mechanism and Machine Theory 35 (1) (2000) 15–40.

Shane E. Jacobs received his Bachelor's of Mechanical Engineering from McGill University in 2004, and his Masters of Aerospace Engineering from the University of Maryland in 2006. He is presently a Ph.D. candidate at the Space Systems Laboratory, in the Department of Aerospace Engineering at the University of Maryland. His research interests are space systems, space human factors, robotics, and space suit design.

David L. Akin is an Associate Professor of Aerospace Engineering and the Director of the Space Systems Laboratory at the University of Maryland. He was the principal investigator for the EASE EVA experiment on STS 61-B, for the ParaShield entry vehicle flight test, and for the Ranger Telerobotic Shuttle Experiment. He has nearly 30 years of experience in EVA and space robotics, focusing on experimental investigations of space operations in neutral buoyancy, and has published over 100 papers in this area.